

PAPER • OPEN ACCESS

## Computer simulation of the formation of digital spectrozonal images

To cite this article: M A Kalitov and N P Kornyshev 2019 *J. Phys.: Conf. Ser.* **1352** 012025

View the [article online](#) for updates and enhancements.



**IOP | ebooks™**

Bringing you innovative digital publishing with leading voices to create your essential collection of books in STEM research.

Start exploring the [collection](#) - download the first chapter of every title for free.

# Computer simulation of the formation of digital spectrozonal images

**M A Kalitov and N P Kornyshev**

Yaroslav-the-Wise Novgorod State University, ul. B. St. Petersburgskaya, 41  
173003 Veliky Novgorod, Russia

E-mail: Nikolai.Kornyshev@novsu.ru

**Abstract.** The article discusses the features of the formation of spectrozonal images corresponding to narrow registration areas by optical and digital means. The processes of the corresponding optical and signal transformations are analyzed. The results of computer simulation are discussed with a view to a qualitative assessment of the degree of consistency between optical spectrozonal visualization and the digital spectrozonal visualization carried out by the differential method. Examples of images of test and real objects obtained by a differential method from the original spectral images are given.

## 1. Introduction

Analysis of spectral images is widely used in such areas as remote sensing of the Earth, medical imaging, forensic science, research of cultural heritage objects, etc. [1–10].

Spectrozone visualization, by analogy with optical and digital image scaling, can be differentiated between optical and digital. If optical spectrozonal visualization involves working directly with the allocated spectrozonal radiant fluxes, digital imaging involves converting (processing) digital copies of the original spectrozonal images in order to generate signals corresponding to the new zones of radiation spectrum registration.

Digital methods of forming multispectral images are of great practical interest, since they allow minimizing the hardware costs for the construction of optical-electronic systems (OES) and expand their functionality.

The above methods are currently being intensively developed and can be classified by the types of mathematical operations with the original spectrozonal images. Thus, in [1–3], differential, integral and differential-integral (combined) methods are distinguished.

By analogy with optical and digital image scaling, which are qualitatively different in that digital scaling introduces certain distortions, in particular, enlargement of pixels and, accordingly, loss of resolution, it is obvious that digital spectral visualization introduces distortions in relation to optical.

Let us consider in more detail the processes of signal conversion when obtaining spectrozonal images and try to formalize their description.

To implement the differential method [2], a pair of spectrozonal images can be obtained either by irradiating an object with light sources with a spectral power  $W_1(\lambda)$  and  $W_2(\lambda)$ , belonging to the corresponding spectral intervals  $\Delta\lambda_1$  and  $\Delta\lambda_2$ , or extracting from the total radiant flux  $W(\lambda)$  the components  $W_1(\lambda)$  and  $W_2(\lambda)$  using optical filters with the corresponding spectral characteristics  $C_1(\lambda)$  and  $C_2(\lambda)$ .



In this case, if  $\Delta\lambda_1 \cap \Delta\lambda_2 \neq 0$ , then the total spectral characteristic of a pair of filters  $C(\lambda) = C_1(\lambda)C_2(\lambda)$ , and if  $\Delta\lambda_1 \cap \Delta\lambda_2 = 0$ , then  $C(\lambda) = 0$ .

The radiant flux  $W(\lambda)$ , which passes through the filters, is respectively divided into  $W_1(\lambda) = C_1(\lambda)W(\lambda)$  and into  $W_2(\lambda) = C_2(\lambda)W(\lambda)$ . These streams are converted by a photodetector into an electrical signal proportional to the brightness of the object [10], respectively:

$$i_1 = \int_{\Delta\lambda_1} W_1(\lambda)G(\lambda)d\lambda \text{ and } i_2 = \int_{\Delta\lambda_2} W_2(\lambda)G(\lambda)d\lambda, \text{ where } G(\lambda) \text{ is the spectral characteristic}$$

of the photodetector.

The frames of the multispectral images  $I_1$  and  $I_2$  are formed by a matrix of  $M \times N$  size elements  $x_n y_m$ ,

$$\text{where } x=1,2..N, y=1,2..M: I_1 = \bigcup_{n=1}^N \bigcup_{m=1}^M i_1(x_n y_m), I_2 = \bigcup_{n=1}^N \bigcup_{m=1}^M i_2(x_n y_m).$$

If the condition  $I_1 \neq 0, I_2 \neq 0, I_1 \neq I_2$  is satisfied, which corresponds to real spectrozonal images, then always the transformations take the form  $\Delta I = I_1 - I_2 \neq 0, I = I_1 I_2 \neq 0$ . Consequently,  $I_1 \cap I_2 \neq 0$ , even if for the corresponding source radiant flux  $\Delta\lambda_1 \cap \Delta\lambda_2 = 0$ .

This means that, in contrast to transformations of directly spectrozonal radiant fluxes, transformations with image-dependent electrical brightness signals that functionally depend on them should result in distortion of the result by “background” components, which appear due to the integral sensitivity of the photodetector.

The images obtained by converting such electrical signals in the case when  $\Delta\lambda_1 \cap \Delta\lambda_2 = 0$ , however, can carry new visual information about the object being visualized with respect to the original spectral images.

In this connection, the formulation of the problem of estimating the degree of these distortions is appropriate. This report discusses the results of a qualitative assessment of the differential method of spectrozonal visualization using computer simulation methods. The essence of this assessment consists in the synthesis of a color image from the RGB components, which are formed by a differential method from four source images obtained in the extended areas of the registration of light fluxes using standard light filters such as yellow light filters (YLF) and red light filters (RLF) [11].

In other words, for the formation of the RGB component, transformations of the form  $B=f(X_b;Y_b)$ ,  $G=f(X_g;Y_g)$ ,  $R=f(X_r;Y_r)$ , are performed, and the correspondence  $X_b \leftrightarrow \text{YLF4}$ ,  $Y_b \leftrightarrow \text{YLF18}$ ,  $X_g \leftrightarrow \text{YLF18}$ ,  $Y_g \leftrightarrow \text{RLF11}$ ,  $X_r \leftrightarrow \text{RLF11}$ ,  $Y_r \leftrightarrow \text{RLF19}$  is observed. In this case, a qualitative assessment of the conformity of digital and optical spectrozonal visualization is reduced to an assessment of the quality of the color rendition of a visualized color object, for example, a test table.

However, as computer modeling shows, directly calculating the difference of two spectrozonal images of the same object, especially in the neighboring registration areas, gives, on the one hand, relatively small values of the difference signal, and on the other hand, some of these values turn out to be negative. Since negative luminance values do not have a physical meaning and can be either not taken into account (discarded) or replaced by the difference modulus, additional distortions of the resulting signal occur.

In this regard, when modeling, it is reasonable to convert the resulting brightness counts using the formulas  $U_{\text{вых } 1}^* = (U_{\text{вых } 1} + U_{\text{макс.}})/2$ ,  $U_{\text{вых } 2}^* = (U_{\text{вых } 2} + U_{\text{макс.}})/2$ , ...  $U_{\text{вых } n}^* = (U_{\text{вых } n} + U_{\text{макс.}})/2$ , where  $U_{\text{вых } .}$  is the difference signal and  $U_{\text{макс.}}$  is its maximum possible value [12], which, on the one hand, eliminates distortion, and on the other hand, increases the average brightness level of the resulting image. After conversion, it is also advisable to use additional brightness correction of the image, and, if necessary, its color correction.

## 2. Results and discussion

As computer modeling shows, when the condition  $\Delta\lambda = \Delta\lambda_1 \cap \Delta\lambda_2 \neq 0$  is fulfilled, the image obtained by optically separating the spectral zone  $\Delta\lambda$  and the resulting image obtained by forming such a zone from a pair of digital spectrozonal images for  $\Delta\lambda_1$  and  $\Delta\lambda_2$  is observed. However, the spectral components in such a resulting digital image are distorted, which leads to differences in their amplitude values from the true values corresponding to the spectral zones formed by an optical path.

So, for example, in the synthesized image obtained by computer modeling, made up of the RGB components obtained by differential, their color matching to the visualized object is observed, however, in this case there is a distortion of color and a decrease in color saturation.

The results of the above transformations are illustrated below. Figure 1 shows a color image of a test object and an image of the R, G, and B components obtained using optical separation.

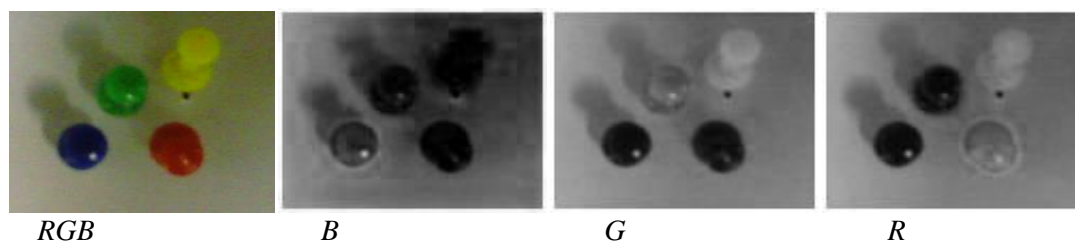


**Figure 1.** Color image of the test object *RGB* and images of the *R*, *G* and *B* components obtained using optical color separation.

Figure 2 shows the spectral characteristics of standard light filters of the YLF and RLF type, highlighting the ranges of 400, 500, 600 and 700 nm, respectively, necessary for forming the R, G and B components by the differential method and obtaining a color image, and in Figure 3 you can see spectral images corresponding to these light filters.

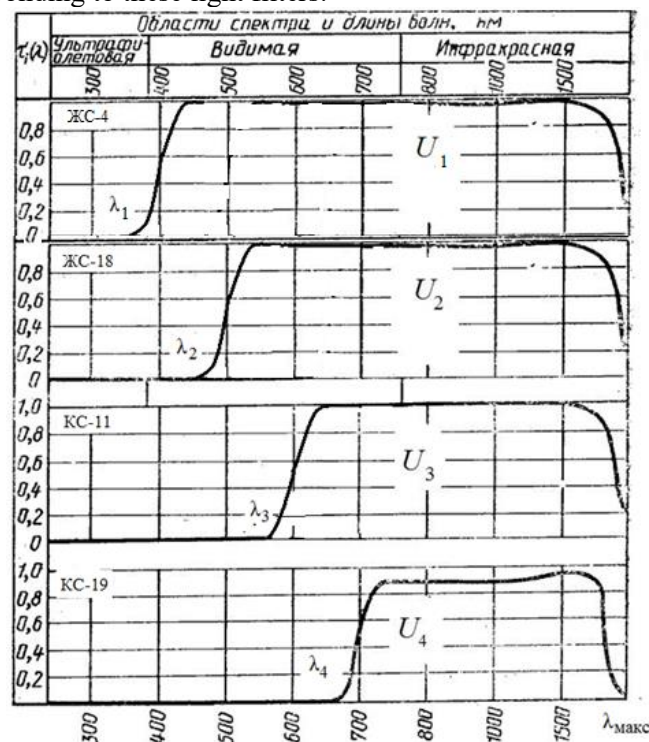


**Figure 2.** Spectral characteristics of standard filters YLF4, YLF18, RLF11, RLF19

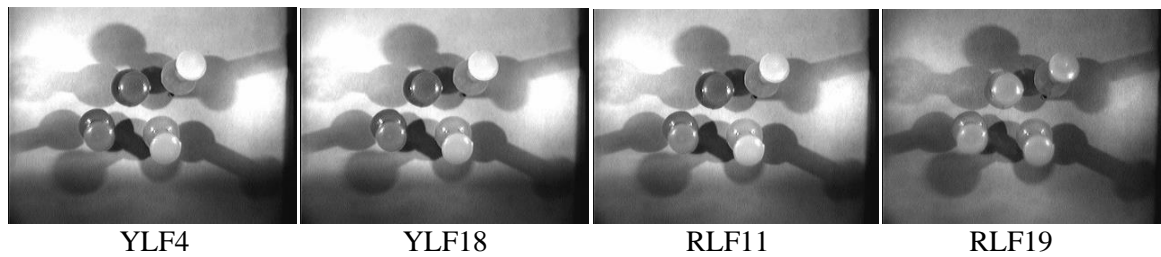


**Figure 3.** Spectrozonal images obtained using standard filters YLF4, YLF18, RLF11, RLF19.

Figure 4 shows the images of the  $R$ ,  $G$  and  $B$  components obtained by the differential method with three different transformation variants and the corresponding synthesized color ( $RGB$ ) images. Figure 5 shows the result of measuring the magnitude of the  $RGB$  component signal at the point of the yellow ball image. As can be seen in Figure 4 and Figure 5, the  $Z_2$  transformation option provides the highest signal level and the best color reproduction and saturation in the synthesized color image compared to the  $Z_1$  and  $Z_3$  transformations.

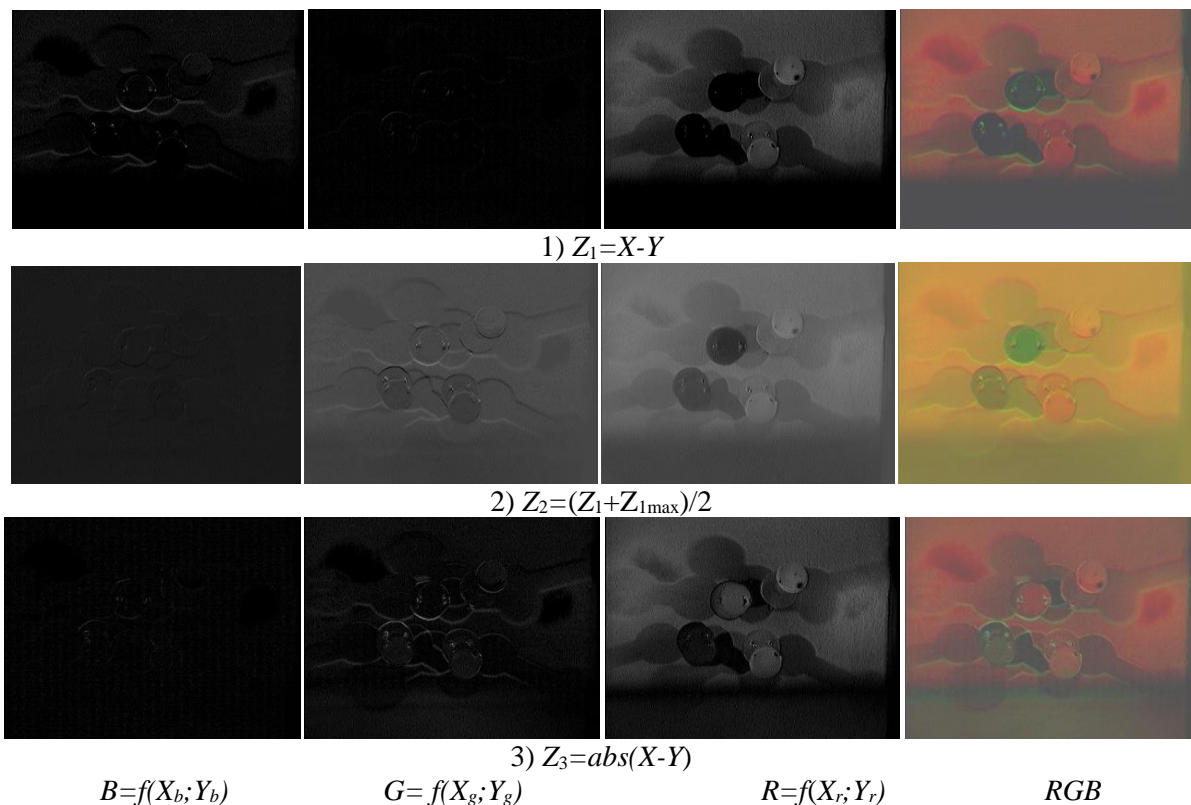


**Figure 4.** Images of the  $R$ ,  $G$ , and  $B$  components obtained by the differential method with three different transformation variants and the corresponding synthesized color ( $RGB$ ) images.

Figure 6 and Figure 7 are examples of differential images of real objects obtained for overlapping ranges  $X(590 \pm 30 \text{ nm})$  and  $Y(625 \pm 30 \text{ nm})$ . As can be seen in the examples, digital differential images carry some new visual information about objects, which can be interpreted as approximately corresponding to a narrow spectral interval, optically extracted.

The differential method can provide some new visual information about objects in the absence of overlapping spectral ranges for a pair of images.

So in Figure 8 and Figure 9 we can see examples of differential images of real objects obtained for non-overlapping ranges  $X(470 \pm 30\text{nm})$  and  $Y(940 \pm 30\text{nm})$ . As we see in the examples, digital differential images have a number of features in detail that cannot be obtained optically.

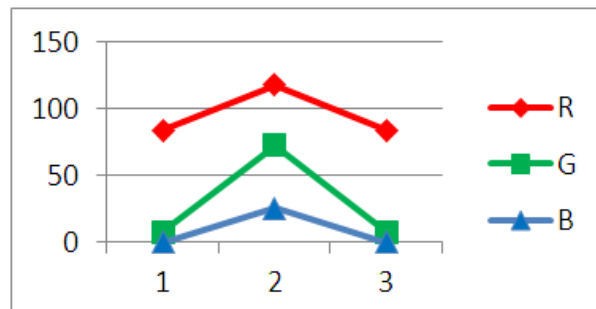


**Figure 5.** The magnitude of the signal component  $R\ G\ B$  for the yellow ball for the three variants of transformations (formulas 1-3).

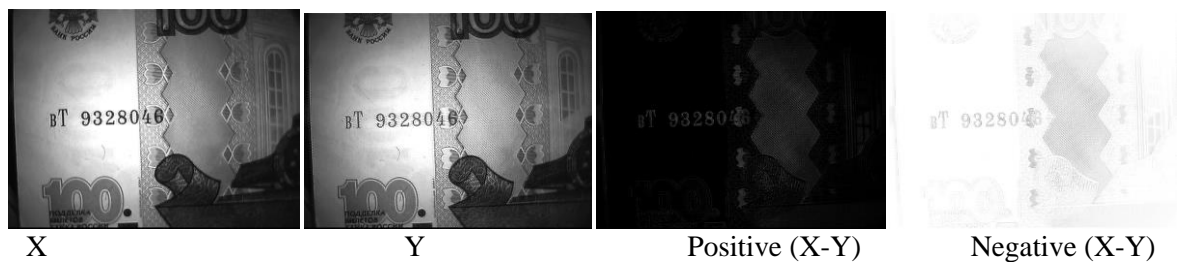


**Figure 6.** A fragment of a 100 Rub bill. X and Y – the original images obtained in overlapping ranges  $X(590 \pm 30\text{nm})$ ,  $Y(625 \pm 30\text{nm})$  and the corresponding differential images in positive and negative.

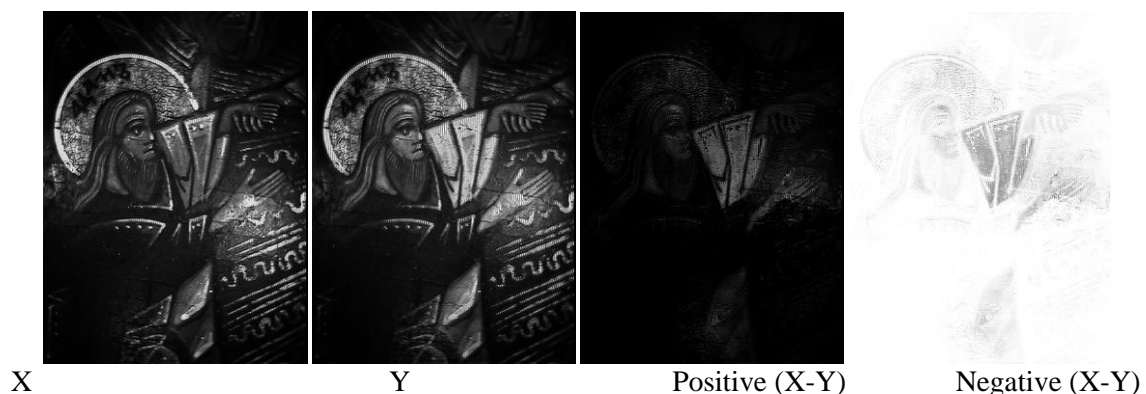


**Figure 7.** Fragment of the icon X and Y - the original images obtained in overlapping ranges  $X(590 \pm 30\text{nm})$ ,  $Y(625 \pm 30\text{nm})$ , and the corresponding differential images in positive and negative.





**Figure 8.** A fragment of a 100 Rub bill. X and Y - the original images obtained in non-overlapping ranges  $X(470 \pm 30\text{nm})$ ,  $Y(940 \pm 30\text{nm})$ , and the corresponding differential images in positive and negative.

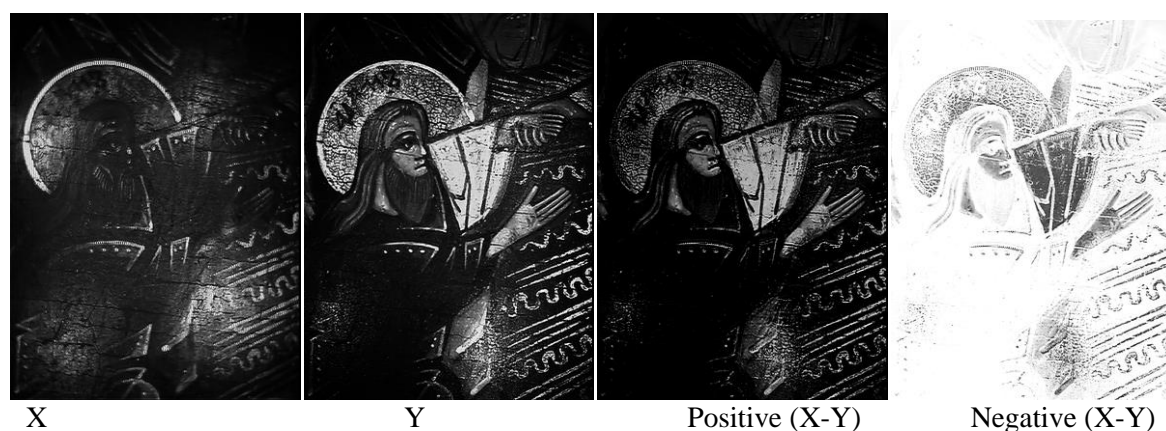


**Figure 9.** Fragment of the icon. X and Y - the original images obtained in non-overlapping ranges  $X(470 \pm 30\text{nm})$ ,  $Y(940 \pm 30\text{nm})$  and the corresponding differential images in positive and negative.

### 3. Conclusion

Digital methods of forming multispectral images allow minimizing the hardware costs for the construction of optical-electronic systems (OES), to expand their functionality, which is of great practical interest.

Computer simulation confirms the compliance of the image obtained by optical selection of the spectral zone with a digital image obtained by the formation of such a zone by a differential method from a pair of spectrozonal images.

At the same time, the spectrozonal components in such a digital image are distorted, which leads to differences in their amplitude values from the true values corresponding to the spectral zones formed optically. At the same time, their color matching to the visualized object is observed, however, at the same time, there is a distortion of color reproduction and a decrease in color saturation.

The differential method can provide new visual information about objects in the absence of overlapping spectral ranges for a pair of images and obtain digital difference images that have a number of features in details that cannot be obtained optically.

### References

- [1] Zubarev Yu B, Sagdullaev Yu S and Sagdullaev T Yu 2009 Spectrozoal methods and systems in space television *Issues of Radioelectronics Television Technology Series Vol 1* 47–64
- [2] Sagdullaev Yu S and Sagdullaev T Yu 2011 To the question of the choice of registration zones in the multispectral television *Issues of Radioelectronics Television Technology Series Vol 2* 20

- [3] Sagdullaev Yu S and Sagdullaev T Yu. 2018 Fundamentals of the construction of information-measuring systems of multispectral television *Issues of Radioelectronics Television Technology Series* Vol **4** 59–67
- [4] Benavides J M, Chang S, Park S et al. 2003 Multispectral digital colposcope for in vivo detection of cervical cancer *Optics Express* **11** 1223–36
- [5] Scheunders P 2001 Local mapping for multispectral image visualization *Image and Vision Computing* Vol **19** 971–978
- [6] Andreeva E V, Butusov V V, Kornyshev N P, Kuzmin V P, Nikitin N S, and Chelpanov V I 2008 Television hardware-software systems for forensic research *Issues of Radioelectronics Television Technology Series* Vol **2** 50–57
- [7] Valero E M et al. 2014 Comparative performance analysis of spectral estimation algorithms and computational optimization of a multispectral imaging system for print inspection *Color Research & Application* Vol **39** 16–27
- [8] Hollaus F, Gau M, and Sablatnig R 2013 Enhancement of multispectral images of degraded documents by employing spatial information *12th International Conference on Document Analysis and Recognition* 145–149
- [9] Kornyshev NP, Lyakhovitsky E A and Rodionov I S 2013 Optical-electronic and television methods and tools in historical paper research of manuscript-book monuments *Photo Image Document* Vol **4** (4) 65–72
- [10] Halfin AM 1955 *Osnovy Televisionnoy Tekhniki* [Fundamentals of Television Equipment] (Moscow: Soviet Radio) 580
- [11] Kornyshev N P, Kalitov MA and Senin A S 2018 Research of the method of differential spectrozone visualization *Bulletin of Novgorod State University Technical Science Series* **1(107)** 62–69
- [12] Kornyshev NP and Kalitov M A 2019 Method for generating digital spectrozone television signals Patent RU 2679921